Resource-Efficient Technologies 3 (2017) 414–421

Contents lists available at ScienceDirect

Resource-Efficient Technologies

journal homepage: www.elsevier.com/locate/reffit

Research paper

Experimental and simulation studies of parabolic trough collector design for obtaining solar energy

Syed Ameen Murtuza[a,*], H.V. Byregowda[b], Mohammed Mohsin Ali H[b], Mohammed Imran[b]

[a] Department of Electrical and Electronics Engineering, Ghousia College of Engineering, VTU, Ramanagaram, Karnataka 562159, India
[b] Department of Mechanical Engineering, Ghousia College of Engineering, VTU, Ramanagaram, Karnataka 562159, India

ARTICLE INFO

Article history:
Received 18 June 2016
Revised 2 March 2017
Accepted 4 March 2017
Available online 18 April 2017

Keywords:
Parabolic trough solar collector
Receiver tube
Solar thermal
Static structural analysis

ABSTRACT

Concentrated solar power has great potential for large scale renewable energy sources, and is currently an eye catching one for its utilization with wide area of improvement. Especially, parabolic trough solar collectors (PTSCs) are gaining popularity due to their increased efficiency as compared to photovoltaics. In this work, an effort has been made to evaluate the performance of a designed 5-m length PTSC model. Heat collecting element was made of stainless steel with water as working fluid. The authentication of the proposed model is justified based on the results obtained on a yearly scale with respect to average inlet and outlet temperatures, surface temperatures and thermal efficiency for the climatic conditions of Ramanagaram. It was observed that March to May yielded better outlet temperatures ranging from 93 °C to 103 °C. Experiments were carried out at different flow rates of 0.4 LPM, 0.8 LPM and 1.2 LPM and corresponding Reynolds number was calculated. It was seen that February to May gave good surface and outlet temperatures as compared with other months while the liquid flow is laminar. Simulation studies were carried out using ANSYS software on receiver tube to ensure the robustness and design effectiveness under static loading conditions.

1. Introduction

One of the most important roles in providing clean non-polluting energy in domestic and industrial applications is played by solar thermal systems. Concentrating solar technologies, such as parabolic dish, compound parabolic collector and parabolic trough, have the ability to operate at high temperatures and are used to supply heat to the industrial process, off-grid electricity and huge electrical power. In a parabolic trough solar collector (PTSC), the reflective profile focuses sunlight on a linear receiver tube or heat collecting element (HCE) through which heat transfer fluid is pumped. This fluid collects the solar energy in the form of heat that can then be used in various applications. Key components of PTSC include the collector structure, the receiver or HCE, the drive system and the fluid circulation system, which conveys thermal energy to its point of use.

The use of concentrating solar energy collectors dates back to the late 19th century. The technology was originally used for pumping water although more unusual applications included a steam-powered printing press demonstrated at the1902 Paris Exposition [1]. It was not until the mid-1970s when large-scale development of PTSCs began in the United States under the Energy Research and Development Administration (ERDA), later the Department of Energy (DOE) (U.S. Department of Energy, 2004). This development was strongly influenced by geopolitical factors, such as the oil crisis, and focused on the provision of industrial process heat rather than electrical power. Typical applications of trough technology included laundry processing, oil refining and steam production for sterilization of medical instruments [2]. The first trough-based Solar Electric Generating Systems (SEGS I) power plant was constructed in 1984 in the U.S. state of California. Eight further plants followed, the last being completed in 1991. Together, SEGS I–IX represent a total of 354 MW of installed electrical capacity and all the plants are still operational. A tenth plant was planned but abandoned when the development company failed to secure financing for construction and went bankrupt (U.S. Depart-

* Corresponding author. Department of Electrical and Electronics Engineering, Ghousia College of Engineering, VTU, Ramanagaram, Karnataka 562159, India. Fax: 080-27273474.
E-mail address: ameen.pse@gmail.com (S.A. Murtuza).

https://doi.org/10.1016/j.reffit.2017.03.003

ment of Energy, 2004). Cheap and stable oil supplies through the 1980s meant no new parabolic trough power.

In recent years, a new momentum in PTSC research has developed, fueled by climate concerns, dwindling oil reserves and political instability in some oil-producing countries. An attractive feature of the technology is that parabolic trough solar collectors are already in use in abundant numbers and research output is likely to find immediate application. Parabolic trough technology has made the crucial leap from pure concept to working solution, offering a real alternative to fossil fuel energy sources. This demonstrated capability gives credibility to trough research, which is now focused on ways to advance PTSC technology and reduce the costs of constructing and operating trough-based power plants.

In the year 2010, Fernandez-Garcia et al. presented an overview of the parabolic trough solar collectors that have been built and marketed in the past century along with a prototype of PTSC under development. It also presents a survey of systems which could integrate this type of concentrating solar system to supply thermal energy up to 400 °C, mainly steam power cycles for electricity generation, as well as examples of each application [3].

A model of trough collector considering new ideas was built using MCNT/mineral oil nanofluid as working fluid with different types of receiver tubes as a significant increase of 11% was achieved on the efficiency of the designed model [4]. Another approach to improve the efficiency was attempted by using molten salt as working fluid [5]. A heat transfer medium with a melting point of 86 °C and a working temperature upper limit of 550 °C was employed. The results depicted that the total heat transfer coefficient of the water to salt heat exchanger ranged between 600 and 1200 W/(m^2-K) for $10{,}000 < Re < 21{,}000$ and $9.5 < Pr < 12.2$. The comparative analysis between the experimental results and empirical correlations demonstrated good performance of low melting point molten salts. In recent studies, Sylthern 800/Al_2O_3 nanofluid was used as working fluid, and a boost of up to 10% on the collector efficiency was observed for an Al_2O_3 concentration of 4% [6].

Experimental characterization of solar parabolic trough collector used in micro-cogeneration systems was carried out. The system produces saturated steam during 8 hrs with a quality higher than 0.6 for a flow rate of 33 kg/hr. The dynamics of the collectors were observed on a cloudy day under two-phase flow, slow strong variations of the output power and flow rate that can even cease with clouds [7].

A comprehensive thermo-optical modeling was proposed to evaluate the performance of a small SPTC with different heat equilibriums in the environment. The developed model is estimated to have a year-round performance assessment with respect to water temperature rise, heat energy generations, optical and thermal efficiencies for climatic conditions of Bhiwani, India [8]. A thermodynamic model framework for low enthalpy process was simulated for SPTC [9]. The simulation results show that in the presence of twisted tape insert, the Nusselt number, the removal factor, the friction factor and the thermal efficiency increase with respect to the empty tube as both twisted ratio and Reynolds number decrease. It was also observed that the enhancement in energy is achieved only when augmentation entropy generation number $N_{s,a} < 1$. If $N_{s,a} > 1$, it is not advisable to use twisted tape insert. In order to facilitate the investigators in the field of parabolic trough solar collector technologies and to highlight the applications such as air heating systems, desalination, industrial purposes and power plants, etc. and their future perspective, a review was carried out which focused on the performance and efficiency of the system [10].

For researchers interested in contributing to the development of PTSCs it is important to be able to test new collector components. To this end, the construction of a parabolic trough collector is vital and a number of such PTSCs have been constructed for research institutions, ranging in size from 1 m^2 to 100 m^2. Smaller-scale PTSCs can be used to test improvements in receiver design, reflective materials, control methods, structural design, thermal storage, testing and tracking methods [11]. One such PTSC with an aperture area of 7.5 m^2 has been developed.

The aim of this study is to test the newly developed PTSC and characterize its performance. This is to be done using a suitable solar collector test standard and comparing the results with a thermal model of the PTSC. The results of this study will allow the performance of new parabolic trough components such as heat collecting elements and surface materials to be measured when the collector becomes a test-rig in an ongoing solar thermal research program.

2. Description of test apparatus

The equipment tested in this study is composed of a locally developed parabolic trough solar collector. The PTSC has a torque-tube structure with a length of 5 m and an aperture width of 1.5 m making a rim angle of 82.2° (Fig. 1). The reflective surface is made of stainless steel sheets covered with aluminized silver reflective film and clamped into the profile formed by parabolic ribs.

Heat collecting element or receiver tube used for testing was made of stainless steel with a diameter of 0.508 m and a length of 5 m to carry the working fluid. The working fluid used was water (Fig. 2).

Table 1 summarizes the key parameters of the parabolic trough solar collector.

The working fluid used is water [12]. 1000 L overhead tank is used to create the potential. A test flow rate of 0.4–1.2 LPM was used to ensure turbulent conditions in the receiver throughout the expected temperature range. Fluid density fluctuations were accommodated during data processing using the water temperature to calculate mass flow rate for each datum point. During testing, flow meter readings were checked by physical measurement. Small variations in mass flow rate were allowed between low and high temperature tests, but properly accounted for in the processing of test data [13].

3. Construction of parabolic trough collector

The development of PTSCs by institutes and universities for research purposes is well documented in the literature. For example Kalogirou [14] describes the design of a trough collector with aperture area of 3.5 m^2, rim angle of 90° and concentration ratio of 21.2. The performance of the collector is reported in terms of the recommended ASHRAE 93 procedure (ASHRAE, 1991) [15]. Literature reports the performance of a multiple-trough collector, consisting of six connected parabolic troughs, each 1.14 m long and 0.12 m wide, giving a total aperture area of 0.82 m^2 [16]. Also successful production steam in the absorber tubes of an existing 29 m long parabolic trough collector with an aperture width 2.5 m and absorber diameter of 25.4 mm is achieved [17]. The construction of a trough with approximately 12 m^2 of aperture area and the capacity to track the sun about two axes was also described in the literature. This was achieved by connecting one end of the parabolic trough to a vertical sliding mechanism and hinged “turret” or pylon [18].

Key aspects of the design and construction of the structure, heat collecting elements and of this PTSC are briefly described here. The primary objective in the design and construction of this collector was to ensure that the reflective surface exhibited a stable, accurate parabolic profile [19]. The basics of parabolic geometry (for example, focal length, rim angle, width and height) are readily available in the literature and are omitted here. Factors

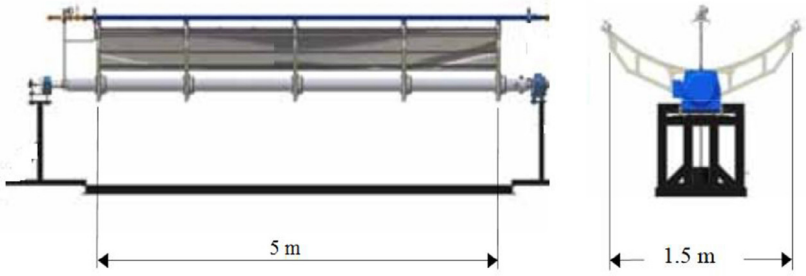

Fig. 1. Parabolic trough collector module.

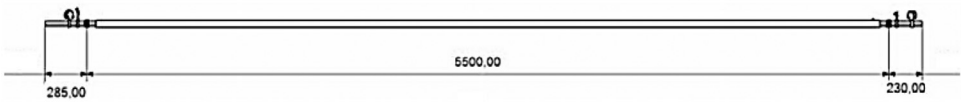

Fig. 2. Receiver tube.

considered in the construction of this PTSC included optical error tolerance, material cost and availability and manufacturing constraints.

Design alternatives for the PTSC structure-type included truss, torque-tube, torque-box, stamped profile and molded fiber-glass structures. The torque-tube structure (Fig. 3) was selected for simplicity and ease of manufacture.

The parabolic ribs were made from mild steel material, to provide the shape of the surface, in order to maintain the strength of the rib. Figures show schematics of the rib, the rib attachment method and the collector structure.

Aluminized silver finished sheet was applied to a stainless steel substrate, which was clamped into the profile formed by the parabolic ribs, producing a stable and sufficiently rigid surface (Fig. 4). The clamping system was designed to allow easy changing of surface sheets for comparative testing of different materials.

The model was designed to ensure the thermal efficacy of the parabolic trough solar collector. The material selection was based on cost, precision needed, machining capability and ease of procurement; major construction was based on MS and aluminum was used for reflective surface for its cost and availability. Teflon bearings were used. Also it was made sure the model is comparable to industrial scale products and suits the requirements.

Installation was done at roof of Haji Nabi Shariff Building for Post-Graduation and Research at Ghousia College of Engineering, Ramanagaram. The site was selected based on favorable wind conditions and the required amount of solar radiations for carrying out the experiment. The other auxiliary instruments used were thermal probe for water temperature measurement, piping and flow control setup, annular tube with CPVC pipe, etc.

The operation of the parabolic trough solar collector with flow condition of different flow rates (0.4 LPM, 0.8 LPM and 1.2 LPM) without tracking was conducted. The readings of water inlet and outlet and surfaces were taken for every 10 minutes from 10:30 am to 3:30 pm to understand the execution of the parabolic trough solar collector.

Analysis was done with the obtained data and the data were analyzed. Static analysis was carried out to obtain the stability of the receiver pipe under static loading condition.

Rise in temperature difference from inlet to outlet is observed experimentally and applied as static thermal load for receiver pipe using ANSYS simulation package. Modeling of the receiver pipe or heat collecting element was done as shown in Fig. 5.

Modeling was followed by meshing which is shown in Fig. 6. Meshing splits our designed components into standard shapes and will calculate the stresses for the standard shapes. Accuracy of the calculations directly depends on more number of shapes provided

Table 1
PTSC key parameters and material properties.

Feature/parameter	Value
Collector dimensions	5.0 m × 1.5 m
Rim angle, ψ_{rim}	82.2°
Absorber diameter, D	28.6 mm
Concentration ratio, C	16.7
Intercept factor, γ	0.823
Surface reflectance, ρ	0.83
Receiver absorptance, α	0.88
Receiver emittance, ε	0.49

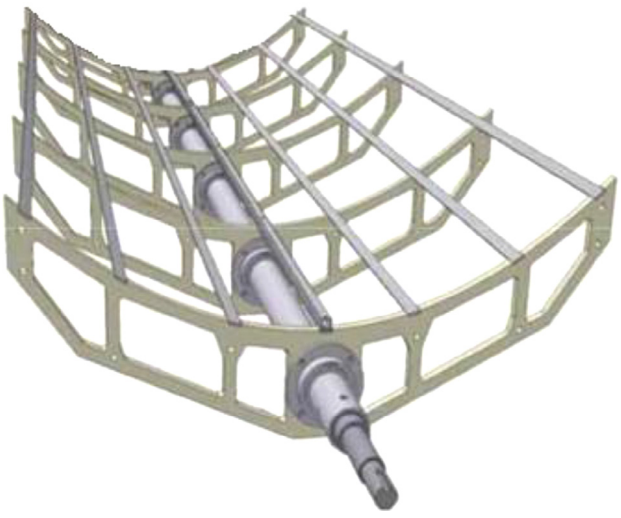

Fig. 3. PTSC torque-tube collector structure with parabolic ribs.

(a) (b)

Fig. 4. Assembly of parabolic trough collector (a) stainless steel substrate prior to installation and (b) assuming parabolic shape.

for simulation. Meshing helps us find the exact weak points and alter our model.

Table 2 describes the properties of elements used for meshing in ANSYS. Tetrahedral type of element division was used in mesh plot for equal number of element division.

The analysis is then followed by calculating the Displacement, von Mises Stress and Thermal Strain to know the safety of the component.

4. Experimental results

Experiments were carried out on scale of 12 months. Avg. temperatures of both inlet water and outlet water were measured. Fig. 7 represents the monthly average minimum and maximum inlet temperatures injected.

Fig. 8 shows the average outlet temperature to the inlet temperature on an annual scale. Significant increase in the temperature was observed in the months of February, March, April and May.

March, April and May gave an acute rise in temperature ranging from 93 °C to 103 °C. Behavior of average surface temperatures of receiver tube in different months is portrayed in Fig. 9.

Experiments were carried out at different flow rates at a range of 0.4 LPM, 0.8 LPM and 1.2 LPM throughout the year and corresponding Reynolds number was calculated. Reynolds number is a dimensionless quantity used to predict flow patterns in different fluid flow situations [20]. For flow in a circular tube of diameter D at an average velocity V, the Reynolds number *Re* is defined as follows:

$$R_e = \frac{\rho DV}{\mu} = \frac{DV}{\nu} \tag{1}$$

Here, μ is the dynamic viscosity of the fluid, and ρ is the density of the fluid. The ratio $\nu = \mu/\rho$ is termed the kinematic viscosity. If the Reynolds number is less than 2000, the flow is called laminar (smooth and constant fluid motion) and if the Reynolds number is more than 4000, it is called turbulent (chaotic flow). If the Reynolds number lies between 2000 and 4000, the flow is known as transition flow (may be laminar or turbulent).

The density of the water (ρ) is 1000 kg/m^3, diameter of the pipe (D) used is 0.0508 m and dynamic viscosity of the water is 8.9×10^{-4} Pa. Table 3 shows the average velocity of the water obtained from flow rate ranges. Flow rate was converted from LPM (liters per minute) to m^3/s and then average velocity V was calculated by the formula

$$V = Q/A \tag{2}$$

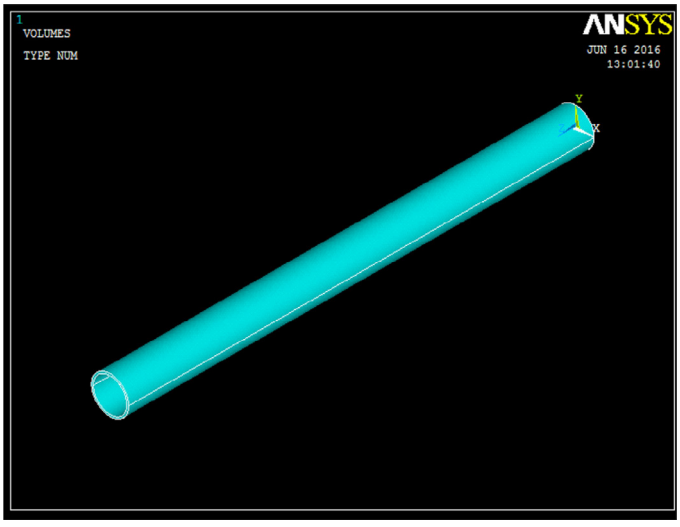

Fig. 5. Modeling of receiver pipe in ANSYS.

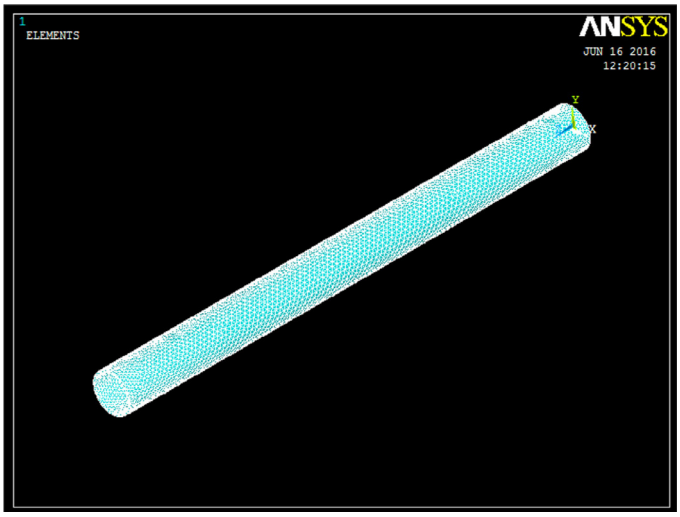

Fig. 6. Mesh plot of receiver pipe in ANSYS.

Table 2
Properties of elements used in meshing.

Type of element	No. of elements	No. of nodes
Solid 183	28,443	9,531

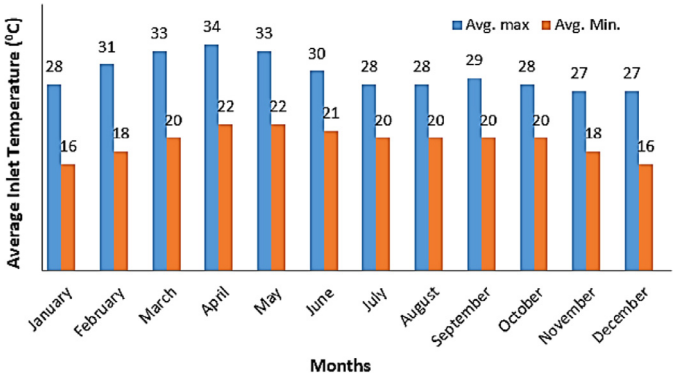

Fig. 7. Average inlet temperature on an annual scale.

where Q is the flow rate in m^3/s and A is the area of cross section of the receiver pipe used and is given by

$$A = \frac{\pi}{4} d^2 = \frac{\pi}{4} (0.0508)^2 = 0.2026\,m^2 \quad (3)$$

Based on the obtained data, the Reynolds number was calculated with respect to the flow rate of the water as shown in Table 4 below.

It is well known fact that better the surface temperature better the results obtained. Table 5 gives the details of surface temperature versus the Reynolds number on an annual scale. It can be clearly seen that February to May were found to have considerably good results as compared to other months.

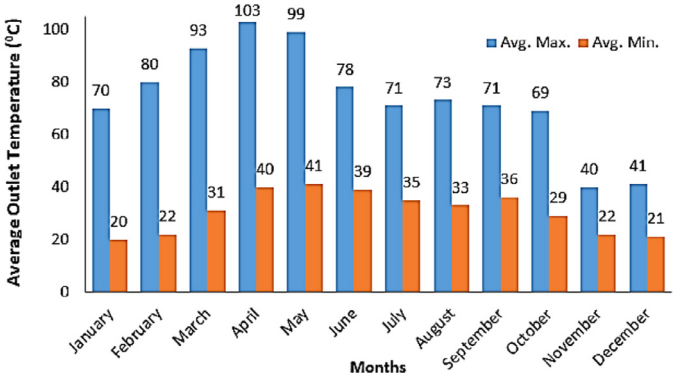

Fig. 8. Average outlet temperature on an annual scale.

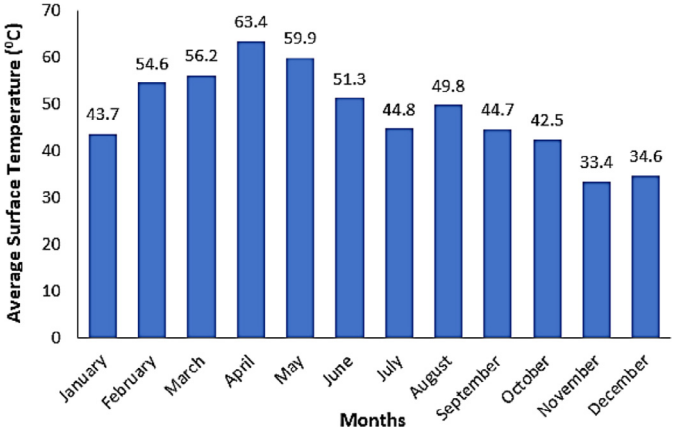

Fig. 9. Average surface temperature on an annual scale.

Table 3
Average velocity of water with respect to flow rate.

Flow rate (LPM)	Flow rate (m^3/s)	Velocity V (m/s)
0.4	6.67E – 06	32.9E – 06
0.8	1.34E – 05	65.84E – 06
1.2	2E – 05	98.71E – 06

Table 4
Reynolds number with respect to flow rate.

Flow rate (LPM)	Reynolds number (Re)	Fluid flow
0.4	1.88E + 03	Laminar
0.8	3.76E + 03	Transitional
1.2	5.63E + 03	Turbulent

Table 5
Annual average surface temperature with respect to the Reynolds number.

Months	Reynolds number		
	1.88E + 03	3.76E + 03	5.63E + 03
January	43.7	38.6	39.3
February	54.6	49.8	40.2
March	56.2	52.1	48.9
April	63.4	61.2	55.4
May	59.9	52.7	50.3
June	51.3	48.5	42.1
July	44.3	38.4	33.2
August	49.8	45.1	39.9
September	44.7	38.4	33.4
October	42.5	35.9	32.4
November	33.4	30.1	28.9
December	34.6	31.1	29

As discussed prior better surface temperature leads to better outlet temperature. The results shown in Table 6 gives detailed elucidation of improvement in outlet temperature with respect to Reynolds number in the months of February, March, April and May, whereas November and December gave very poor results.

Thermal efficiency (η) [15] at different Reynolds number was calculated on an annual scale by

$$\eta = \frac{T_{out} - T_{in}}{T_{out}} \times 100 \quad (4)$$

where T_{out} is the average outlet temperature and T_{in} is the average inlet temperature.

The efficiency versus Reynolds number plots are shown in Table 7.

Table 6
Annual average outlet temperature with respect to the Reynolds number.

Months	Reynolds number		
	1.88E + 03	3.76E + 03	5.63E + 03
January	70	42.7	20
February	80	49.4	22
March	93	61.7	31
April	103	69.9	40
May	99	68.7	41
June	78	56.5	39
July	71	51.2	35
August	73	51.4	33
September	71	52.1	36
October	69	47.2	29
November	40	29.9	22
December	41	30.1	21

Table 7
Annual thermal efficiency versus Reynolds number.

Months	Reynolds number		
	1.88E+03	3.76E+03	5.63E+03
January	70	42.7	20
February	80	49.4	22
March	93	61.7	31
April	103	69.9	40
May	99	68.7	41
June	78	56.5	39
July	71	51.2	35
August	73	51.4	33
September	71	52.1	36
October	69	47.2	29
November	40	29.9	22
December	41	30.1	21

Maximum efficiency was obtained in the month of May at the Reynolds number of 1.88E+03. It was also observed from the results obtained (from Figs. 8–10) that when fluid flow is laminar better the results are achieved.

5. Simulation results

Static structural analysis of the receiver tube was done using ANSYS simulation package in order to check the robustness of the receiver tube. Fig. 10 illustrates the simulation model of the receiver tube at a thermal loading of 63 °C temperature difference in the month of April. The month of April is shown below as an example for the reason that it gives maximum thermal loading as compared to other months. However, the analysis was done on the receiver tube at different thermal loadings obtained annually. Simulation of static structural analysis was effectuated for three different parameters such as Displacement, von Mises Stress and Thermal Strain.

The results in Fig. 10(a) shows that 0.20109 mm of maximum displacement in the receiver tube of the PTSC shall be attained under the thermal loading of 63 °C in month of April. The maximum von Mises Stresses on the receiver tube were observed to be 208.779 MPa (Fig. 10(b)). The maximum Thermal Strain (Fig. 10(c)) on the receiver tube was found to be 0.001178. All the values obtained were under their theoretical limits and hence less stresses were found in the usage of the material of the receiver pipe. The material used for the receiver pipe was stainless steel (SS). It was used because of its properties of thermal conductivity, specific heat, thermal elongation as a function of temperature, etc., and is very much desirable and preferable to be used as a receiver tube in a parabolic trough solar collector [21].

Static structural analysis of the receiver pipe was done on a scale of a year using ANSYS simulation environment. Based on the result obtained from the simulation the results are inferred. Table 8 gives a detailed explanation of different parameters measured in a span of a year.

The displacement of the SS receiver tube on various values of thermal loadings obtained in different months is clearly depicted in Table 8. The maximum value of displacement obtained in the month of April was 0.20109 mm and the minimum in the month of December was 0.006384 mm.

von Mises stress is used to check whether their design will withstand a given loading condition. If the maximum value of von Mises stress induced in the material is more than the strength of the material, then the material will fail. The standard yielding strength of stainless steel material is 215 MPa [22]. Therefore, von Mises stress analysis was indeed very much essential for the assurance of the strength of the material. Table 8 shows the variation of von Mises stress on the receiver pipe with respect to the thermal

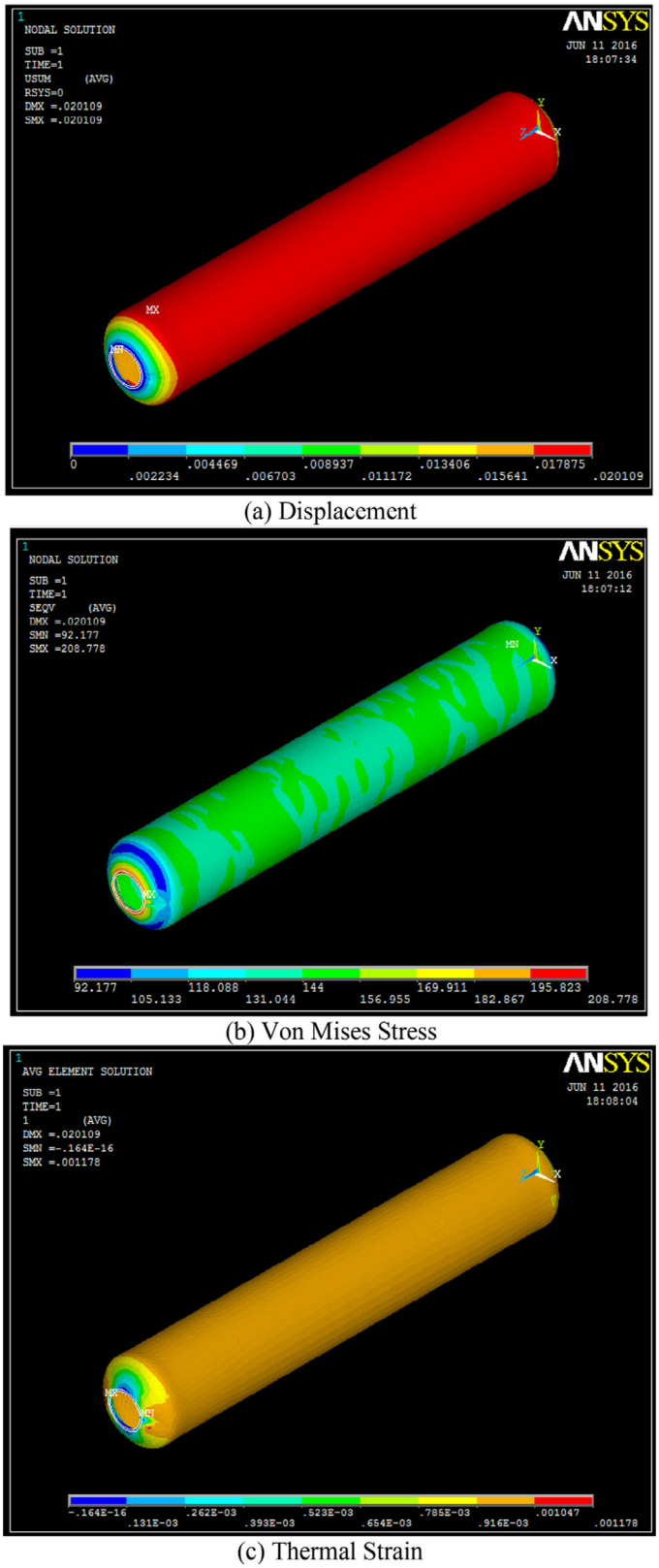

Fig. 10. Simulation results of the receiver pipe in the month of April: (a) Displacement, (b) von Mises Stress and (c) Thermal Strain.

Table 8
Statistical analysis parameters measured in a span of a year.

Months	Thermal loading (°C)	Displacement (mm)	von Mises Stress (MPa)	Thermal Strain	Factor of safety (FoS)
January	50	0.1596	165.697	9.35E – 04	1.297549
February	58	0.18513	192.209	0.001084	1.118574
March	62	0.1979	205.464	0.001159	1.046412
April	63	0.20109	208.779	0.001178	1.029797
May	58	0.18513	192.209	0.001084	1.118574
June	39	0.12449	129.244	7.29E – 04	1.663520
July	36	0.11491	119.302	6.73E – 04	1.802149
August	40	0.12768	132.558	7.48E – 04	1.621932
September	35	0.11172	115.988	6.54E – 04	1.853640
October	40	0.12768	132.558	7.48E – 04	1.621932
November	22	0.007022	72.907	4.11E – 04	2.948962
December	20	0.006384	66.279	3.74E – 04	3.243863

loading provided in different months. The maximum value of the von Mises Stress obtained was 208.779 MPa in the month of April and 66.279 MPa in the month of December. The stresses were observed within the strength of the material.

Eventually, thermal strain was also calculated in order to check the chance of the receiver pipe to change the shape, area or volume with respect to the change in temperature supplied. Table 8 clearly shows that the values of thermal strain are small. The thermal strain at its maximum was found to be about 0.001178 in the month of April and minimum was 0.374E – 04 in the month of December. Thus it established the robustness, sturdiness and healthiness of the receiver tube, especially the material used.

Factor of safety (FoS) was also calculated to ensure capacity of a material beyond actual load. Essentially, the factor of safety is how much stronger the material is than it usually needs to be for an intended load. The factor of safety [13,19] is measured using the formula as depicted in Equation (5)

$$\eta = \frac{\sigma_y}{\sigma_{calc}} \tag{5}$$

where σ_y is the yielding strength of the stainless steel material which is 215 MPa and σ_{calc} is von Mises Stress value (Calculated Stress using ANSYS). Table 8 gives the factor of safety under obtained von Mises stress in different months. The standard value for factor of safety is 1.85 for stainless steel [21]. Hence the results obtained are satisfying since all the values obtained are around 1.85.

6. Conclusions

A 5 m length PTSC was designed in reference to the literature available along with the local techniques to overcome hardships. Torque tube design has been very robust and effective in order to take-up the load of the mild steel ribs assembly in order to accommodate the aluminum sheets for reflection. The design and fabrication were done successfully and the performance of the designed parabolic trough solar collector is satisfactory.

Modeling of receiver pipe or heat collecting element was done using ANSYS simulation package under static loading conditions to ensure the robustness of the design. 0.20109 mm of maximum displacement was observed under the thermal loading of 63 °C in the month of April. The von Mises stress on the receiver tube was observed to be 208.779 MPa and the thermal strain was found to be 0.001178. The factor of safety (FoS) was also calculated to ensure the capacity of a material beyond actual load for a scale of a year and results obtained were quite satisfactory.

The experiments were carried out on a scale of 12 months. Average temperatures of both inlet water and outlet water were measured. February to May gave significantly good temperatures from 80 °C to 103 °C. Reynolds number with respect to different flows such as 0.4 LPM, 0.8 LPM and 1.2 LPM was calculated in order to predict flow pattern in the receiver tube. Plots of surface temperature, outlet temperature and thermal efficiency versus Reynolds number on a scale of 12 months were used and it was observed that better results were obtained in the months March, April and May with laminar flow.

6.1. Future scope

The design of the parabolic torque-tube collector structure with rib design used mild steel as the material, which provides good mechanical strength but accounts for the increase in the weight of the overall collector. Hence an advanced metal matrix composite shall be proposed which may overcome these drawbacks. Also the design uses water as working fluid, this can be replaced by molten salts as they may provide better heat transfer properties as compared to water. Different combinations of carbonates–nitrates–chlorides may be used and experiments can be conducted for its validation for future work.

Acknowledgement

The authors acknowledge Ghousia College of Engineering, Ramanagaram – 562159, Karnataka, India for providing the resources intended for conducting the experiments.

References

[1] J.A. Duffie, W.A. Beckman, Solar Engineering of Thermal Processes, John Wiley & Sons, Inc, New York, 1991.
[2] W.B. Stine, R.W. Harrigan, Solar Energy Fundamentals and Design with Computer Applications, John Wiley & Sons, Inc, New York, 1985.
[3] A. Fernandez-Garcia, E. Zarza, L. Valenzuela, M. Perez, Parabolic-trough solar collectors and their applications, Renew. Sustain. Energy Rev 1 (7) (2010) 1695–1721.
[4] A. Kasaeian, S. Daviran, R.D. Azarian, A. Rashidi, Performance evaluation and nanofluid using capability study of a solar parabolic trough collector, Energy Convers. Manag 89 (2015) 368–375.
[5] Y.-T. Wu, S.-W. Liu, Y.-X. Xiong, C.-F. Ma, Y.-L. Ding, Experimental study on the heat transfer characteristics of a low melting point salt in a parabolic trough solar collector system, Appl. Therm. Eng 89 (2015) 748–754.
[6] J.-L. Bouvier, G. Michaux, P. Salagnac, F. Nepveu, D. Rochier, T. Kientz, Experimental characterisation of a solar parabolic trough collector used in a micro-CHP (micro-cogeneration) system with direct steam generation, Energy 83 (2015) 474–485.
[7] D. Kumar, S. Kumar, Year-round performance assessment of a solar parabolic trough collector under climatic condition of Bhiwani, India: a case study, Energy Convers. Manag 106 (2015) 224–234.
[8] O.A. Jaramillo, M. Borunda, K.M. Velazquez-Lucho, M. Robles, Parabolic trough solar collector for low enthalpy processes: an analysis of the efficiency enhancement by using twisted tape inserts, Renew Energy 93 (2016) 125–141.
[9] E. Kaloudis, E. Papanicolaou, V. Belessiotis, Numerical simulations of a parabolic trough solar collector with nanofluid using a two-phase model, Renew Energy 97 (2016) 218–229.
[10] V.K. Jebasingh, G.M. Joselin Herbert, A review of solar parabolic trough collector, Renew. Sustain. Energy Rev 54 (2016) 1085–1091.

[11] A. Thomas, Simple structure for parabolic trough concentrator, Energy Convers. Manage 35 (7) (1994) 569–573.
[12] M.J. Brooks, I. Mils, T.M. Harms, Performance of a parabolic trough solar collector, J. Energy South. Afr 17 (2005) 71–80 Southern Africa.
[13] R.F. Budynas, J.K. Nisbett, Shigley's Mechanical Design, 9th ed., Mc Graw Hill, New York, 2011.
[14] S. Kalogirou, Parabolic trough collector system for low temperature steam generation: design and performance characteristics, Appl. Energy 55 (1996) 1–19.
[15] ASHARE, Method of Testing to Determine the Thermal Performance of Solar Collectors, ASHARE Standards, No. 93 – 1986, American Society of Heating, Atlanta, 1986.
[16] S.M.A. Ibrahim, The forced circulation performance of a sun tracking parabolic concentrator collector, in: Proceedings of the World Renewable Energy Congress, 1996, pp. 568–571.
[17] R. Almanza, A. Lentz, G. Jimenez, Receiver behaviour in direct steam generation with parabolic troughs, Sol. Energy 61 (4) (1997) 275–278.
[18] G.C. Bakos, D. Adamopoulus, M. Soursos, N.F. Tsagas, Design and construction of a line focus parabolic trough solar concentrator for electricity generation, Proceedings of ISES Solar World Congress, Vol. III, Elsevier, Jerusalem, 1999, pp. 315–323.
[19] J.E. Shigley, C.R. Mischke, Mechanical Engineering Design (in SI Units), 6th ed., Tata Mc Graw Hill, New Delhi, 1986.
[20] R.K. Bansal, A Textbook of Fluid Mechanics and Hydraulic Machines, Laxmi Publications, New Delhi, 2006.
[21] J.R. Davis, ASM Specialty Handbook Stainless Steel, ASM International-The Materials Information Society, Ohio, 1994.
[22] J.E. Shigley, Mechanical Engineering Design Data Handbook, vol. 1, McGraw-Hill Companies, New York, 1996.